Explorations of New Second-Order NLO Materials in the Potassium Vanadyl Iodate System

Chuan-Fu Sun,[a,b] Chun-Li Hu,[a] Xiang Xu,[a] Bing-Ping Yang,[a] Jiang-Gao Mao*[a]

Supporting Information

Table S1. Calculation of dipole moment for IO_3, VO_6 or VO_5 polyhedra and net dipole moment for a unit cell in four compounds.

Table S2. The state energies (eV) of the lowest conduction band (L-CB) and the highest valence band (H-VB) of α-$KVO_2(IO_3)_2(H_2O)$, β-$KVO_2(IO_3)_2(H_2O)$, $K_4[(VO)(IO_3)_5]_2(HIO_3)(H_2O)_2{\cdot}H_2O$, and $K(VO)_2O_2(IO_3)_3$.

Table S3. The experimental and calculated gaps as well as the scissor values adopted in the optical properties calculations.

Table S4. The calculated bond orders of α-$KVO_2(IO_3)_2(H_2O)$, β-$KVO_2(IO_3)_2(H_2O)$, $K_4[(VO)(IO_3)_5]_2(HIO_3)(H_2O)_2{\cdot}H_2O$, and $K(VO)_2O_2(IO_3)_3$.

Table S5. The angles between the crystallography axes (i.e. *a*, *b* and *c*) and the principal dielectric axes (i.e. x, y and z) in triclinic crystal $K_4[(VO)(IO_3)_5]_2(HIO_3)(H_2O)_2{\cdot}H_2O$.

Figure S1. Experimental and simulated powder X-ray diffraction data for α-$KVO_2(IO_3)_2(H_2O)$, β-$KVO_2(IO_3)_2(H_2O)$, $K_4[(VO)(IO_3)_5]_2(HIO_3)(H_2O)_2{\cdot}H_2O$, $K(VO)_2O_2(IO_3)_3$, and $M[(VO)_2(IO_3)_3O_2]$ ($M = Rb^+, Cs^+, NH_4^+$).

Figure S2. Powder X-ray diffraction studies for the thermal decomposition products of α-$KVO_2(IO_3)_2(H_2O)$, β-$KVO_2(IO_3)_2(H_2O)$, $K_4[(VO)(IO_3)_5]_2(HIO_3)(H_2O)_2{\cdot}H_2O$, and $K(VO)_2O_2(IO_3)_3$.

Figure S3. The infrared spectra of α-$KVO_2(IO_3)_2(H_2O)$, β-$KVO_2(IO_3)_2(H_2O)$, $K_4[(VO)(IO_3)_5]_2(HIO_3)(H_2O)_2{\cdot}H_2O$, and $K(VO)_2O_2(IO_3)_3$.

Figure S4. UV absorption spectra of $K(VO)_2O_2(IO_3)_3$ and $M[(VO)_2(IO_3)_3O_2]$ (M = Rb^+, Cs^+, NH_4^+).

Figure S5. Optical diffuse reflectance spectra for $M[(VO)_2(IO_3)_3O_2]$ (M = Rb^+, Cs^+, NH_4^+).

Figure S6. Polarization versus applied electric field for $K_4[(VO)(IO_3)_5]_2(HIO_3)(H_2O)_2{\cdot}H_2O$ and $K(VO)_2O_2(IO_3)_3$.

Figure S7. Calculated band structures of α-$KVO_2(IO_3)_2(H_2O)$, β-$KVO_2(IO_3)_2(H_2O)$, $K_4[(VO)(IO_3)_5]_2(HIO_3)(H_2O)_2{\cdot}H_2O$, and $K(VO)_2O_2(IO_3)_3$.

Figure S8. Electronic density of states of α-$KVO_2(IO_3)_2(H_2O)$, β-$KVO_2(IO_3)_2(H_2O)$, $K_4[(VO)(IO_3)_5]_2(HIO_3)(H_2O)_2{\cdot}H_2O$, and $K(VO)_2O_2(IO_3)_3$.

Figure S9. The imaginary part of the dielectric function polarized, average imaginary part and real part of the dielectric function over three dielectric axes directions for β-$KVO_2(IO_3)_2(H_2O)$, $K_4[(VO)(IO_3)_5]_2(HIO_3)(H_2O)_2{\cdot}H_2O$, and $K(VO)_2O_2(IO_3)_3$.

Figure S10. Calculated linear refractive indices for β-$KVO_2(IO_3)_2(H_2O)$, $K_4[(VO)(IO_3)_5]_2(HIO_3)(H_2O)_2{\cdot}H_2O$, and $K(VO)_2O_2(IO_3)_3$.

Figure S11. Calculated frequency-dependent second harmonic generation coefficients for β-$KVO_2(IO_3)_2(H_2O)$, $K_4[(VO)(IO_3)_5]_2(HIO_3)(H_2O)_2{\cdot}H_2O$, and $K(VO)_2O_2(IO_3)_3$.

Figure S12. Calculated frequency-dependent second harmonic generation coefficients for $Rb[(VO)_2(IO_3)_3O_2]$, $Cs[(VO)_2(IO_3)_3O_2]$, and $NH_4[(VO)_2(IO_3)_3O_2]$.

Table S1. Calculation of dipole moment for IO_3, VO_6 or VO_5 polyhedra and net dipole moment for a unit cell in four compounds (D = Debyes, K^+ ions and water molecules were not considered).

α-$KVO_2(IO_3)_2(H_2O)$				
Polar unit	Dipole moment (D)			
	total magnitude	*x*-component	*y*-component	*z*-component
$I(1)O_3$	14.52	11.63	8.25	2.75
$I(2)O_3$	14.33	3.93	1.51	13.70
$V(1)O_6$	7.64	1.75	6.43	3.74
Net dipole moment (a unit cell)	0	0	0	0
β-$KVO_2(IO_3)_2(H_2O)$				
Polar unit	Dipole moment (D)			
	total magnitude	*x*-component	*y*-component	*z*-component
$I(1)O_3$	14.29	9.85	4.94	9.10
$I(2)O_3$	16.59	15.27	4.27	4.89
$V(1)O_5$	3.05	1.75	0.52	2.44
Net dipole moment (a unit cell)	0	0	0	0
$K_4[(VO)(IO_3)_5]_2(HIO_3)(H_2O)_2{\cdot}H_2O$				
Polar unit	Dipole moment (D)			
	total magnitude	*x*-component	*y*-component	*z*-component
$I(1)O_3$	13.84	7.19	11.43	3.02
$I(2)O_3$	13.77	8.26	10.93	1.42
$I(3)O_3$	14.53	10.38	0.53	10.15
$I(4)O_3$	15.24	10.22	11.27	0.88
$I(5)O_3$	15.19	4.08	11.51	9.04
$I(6)O_3$	14.64	10.16	1.45	10.44
$I(7)O_3$	13.23	8.67	9.70	2.40
$I(8)O_3$	16.01	7.59	8.05	11.58
$I(9)O_3$	15.75	11.96	10.24	0.45
$I(10)O_3$	15.61	3.86	11.09	10.29
$I(11)O_3$	14.48	9.73	9.58	4.81
$V(1)O_6$	5.34	2.42	3.33	3.41
$V(2)O_6$	5.89	1.97	4.48	3.29
Net dipole moment (a unit cell)	33.62	10.21	29.65	12.13
$K(VO)_2O_2(IO_3)_3$				
Polar unit	Dipole moment (D)			
	total magnitude	*x*-component	*y*-component	*z*-component
$I(1)O_3$	14.77	0	14.53	2.67
$I(2)O_3$	13.36	1.08	4.35	12.59
$V(1)O_6$	5.86	0.71	5.36	2.26
Net dipole moment (a unit cell)	129.48	0	0	129.48

Table S2. The state energies (eV) of the lowest conduction band (L-CB) and the highest valence band (H-VB) of four compounds.

Compound	k-point	L-CB	H-VB
α-$KVO_2(IO_3)_2(H_2O)$	*G* (0.000, 0.000, 0.000)	2.66488	0
	Z (0.000, 0.000, 0.500)	2.66845	-0.01174
	T (-0.500, 0.000, 0.500)	2.70478	-0.14669
	Y (-0.500, 0.000, 0.000)	2.7043	-0.14421
	S (-0.500, 0.500, 0.000)	2.74928	-0.25308
	X (0.000, 0.500, 0.000)	2.70825	-0.16563
	U (0.000, 0.500, 0.500)	2.72001	-0.18451
	R (-0.500, 0.500, 0.500)	2.74791	-0.25233
β-$KVO_2(IO_3)_2(H_2O)$	*G* (0.000, 0.000, 0.000)	2.53857	-0.01155
	Z (0.000, 0.000, 0.500)	2.56016	-0.01754
	T (-0.500, 0.000, 0.500)	2.70158	-0.07596
	Y (-0.500, 0.000, 0.000)	2.69509	-0.07305
	S (-0.500, 0.500, 0.000)	2.76193	-0.0757
	X (0.000, 0.500, 0.000)	2.51134	0
	U (0.000, 0.500, 0.500)	2.51232	-5.99739E-4
	R (-0.500, 0.500, 0.500)	2.76345	-0.08197
$K_4[(VO)(IO_3)_5]_2(HIO_3)(H_2O)_2{\cdot}H_2O$	*G* (0.000, 0.000, 0.000)	2.00117	0
	F (0.000, 0.500, 0.000)	1.99736	-0.04061
	Q (0.000, 0.500, 0.500)	1.99847	-0.03874
	Z (0.000, 0.000, 0.500)	2.001	-0.00593
	G (0.000, 0.000, 0.000)	2.00117	0
$K(VO)_2O_2(IO_3)_3$	*T* (0.500, -0.500, 0.000)	1.83457	-0.06669
	W (0.750, -0.250, -0.250)	1.87833	-0.24323
	R (0.500, 0.000, 0.000)	1.76989	-0.08523
	G (0.000, 0.000, 0.000)	1.96209	-0.09799
	X (0.500, -0.500, -0.500)	1.67255	-0.00201

Table S3. The experimental and calculated gaps as well as the scissor values adopted in the optical properties calculations.

	Eg(exp.)(eV)	Eg(cal.) (eV)	Scissors (eV)
β-$KVO_2(IO_3)_2(H_2O)$	3.39	2.51	0.88
$K_4[(VO)(IO_3)_5]_2(HIO_3)(H_2O)_2{\cdot}H_2O$	2.27	2.00	0.27
$K(VO)_2O_2(IO_3)_3$	2.30	1.67	0.63
$Rb[(VO)_2(IO_3)_3O_2]$	2.35	1.61	0.74
$Cs[(VO)_2(IO_3)_3O_2]$	2.47	1.60	0.87
$NH_4[(VO)_2(IO_3)_3O_2]$	2.43	1.56	0.87

Table S4. The calculated bond orders of the four compounds.

α-$KVO_2(IO_3)_2(H_2O)$					
Bond	Bond length	Bond order	Bond	Bond length	Bond order
V-O	1.6283	0.91	V-O	1.6613	0.80
V-O	1.9580	0.42	V-O	2.0056	0.36
V-O	2.1832	0.25	V-O	2.1735	0.24
I-O	1.7786	0.48	I-O	1.7820	0.38
I-O	1.8015	0.37	I-O	1.8633	0.30
I-O	1.8188	0.26	I-O	1.8566	0.20
β-$KVO_2(IO_3)_2(H_2O)$					
Bond	Bond length	Bond order	Bond	Bond length	Bond order
V-O	1.6186	0.93	V-O	1.6182	0.90
V-O	1.9593	0.38	V-O	2.0138	0.33
V-O	2.02583	0.33	I-O	1.7748	0.45
I-O	1.7769	0.44	I-O	1.7868	0.44
I-O	1.8328	0.28	I-O	1.8426	0.20
I-O	1.8636	0.18			
$K_4[(VO)(IO_3)_5]_2(HIO_3)(H_2O)_2{\cdot}H_2O$					
Bond	Bond length	Bond order	Bond	Bond length	Bond order
V-O	1.5866	0.94	V-O	1.5934	0.92

V-O	1.8932	0.45	V-O	1.8935	0.44
V-O	1.8922	0.43	V-O	1.8916	0.40
V-O	1.9144	0.42	V-O	1.9202	0.41
V-O	1.9147	0.40	V-O	1.9751	0.39
V-O	2.1966	0.28	V-O	2.1707	0.25
I-O	1.8082	0.56	I-O	1.7903	0.47
I-O	1.7912	0.47	I-O	1.8134	0.46
I-O	1.8012	0.46	I-O	1.7830	0.45
I-O	1.8084	0.44	I-O	1.7969	0.43
I-O	1.7846	0.42	I-O	1.7946	0.41
I-O	1.8150	0.41	I-O	1.8430	0.41
I-O	1.8035	0.40	I-O	1.8046	0.40
I-O	1.7901	0.39	I-O	1.7980	0.36
I-O	1.8112	0.36	I-O	1.7858	0.35
I-O	1.7980	0.35	I-O	1.8111	0.35
I-O	1.8161	0.35	I-O	1.8153	0.33
I-O	1.8188	0.29	I-O	1.8223	0.29
I-O	1.8592	0.23	I-O	1.8870	0.21
I-O	1.8833	0.17	I-O	1.8935	0.17
I-O	1.8981	0.17	I-O	1.8841	0.15
I-O	1.8599	0.15	I-O	1.8671	0.12
$K(VO)_2O_2(IO_3)_3$					
Bond	Bond length	Bond order	Bond	Bond length	Bond order
V-O	1.6229	0.92	V-O	1.8801	0.55
V-O	1.8792	0.53	V-O	1.9317	0.39
V-O	1.9671	0.37	V-O	2.2019	0.23
I-O	1.7719	0.50	I-O	1.7811	0.44
I-O	1.8290	0.29	I-O	1.8485	0.27
I-O	1.8541	0.23			

Table S5. The angles between the crystallography axes (i.e. *a*, *b* and *c*) and the principal dielectric axes (i.e. x, y and z) in triclinic crystal $K_4[(VO)(IO_3)_5]_2(HIO_3)(H_2O)_2 \cdot H_2O$.

□	*a*-O-x	*b*-O-x	*c*-O-x	*a*-O-y	*b*-O-y	*c*-O-y	*a*-O-z	*b*-O-z	*c*-O-z
Angle(°)	20.55	74.16	91.52	98.60	36.62	130.50	108.51	57.97	40.54

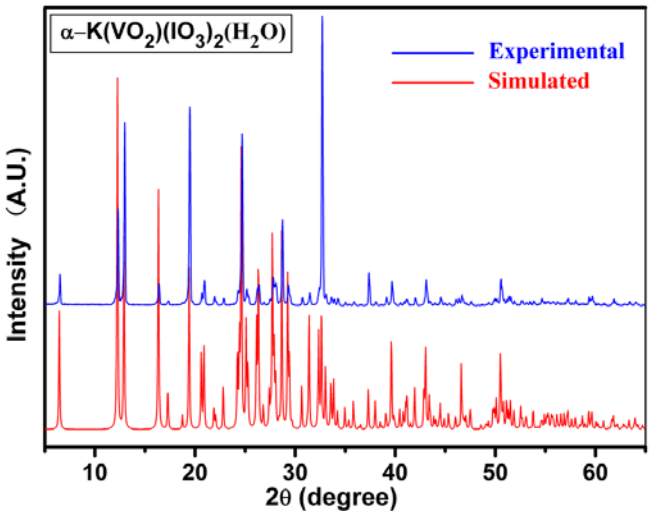
α–K(VO2)(IO3)2(H2O)
Experimental
Simulated
Intensity (A.U.)
10
20
30
40
50
60
2θ (degree)

(a)

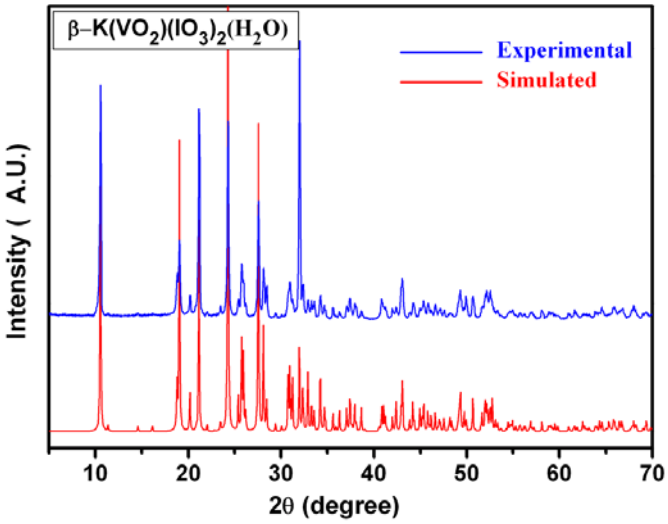
β–K(VO2)(IO3)2(H2O)
Experimental
Simulated
Intensity (A.U.)
10
20
30
40
50
60
70
2θ (degree)

(b)

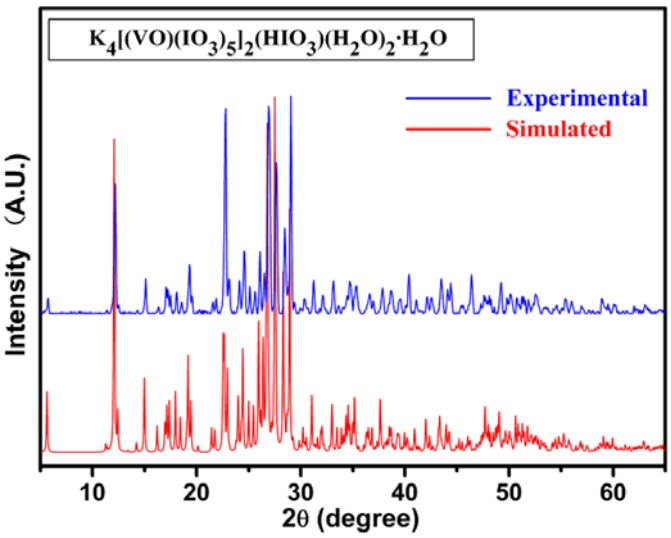
K4[(VO)(IO3)5]2(HIO3)(H2O)2·H2O
Experimental
Simulated
Intensity (A.U.)
10
20
30
40
50
60
2θ (degree)

(c)

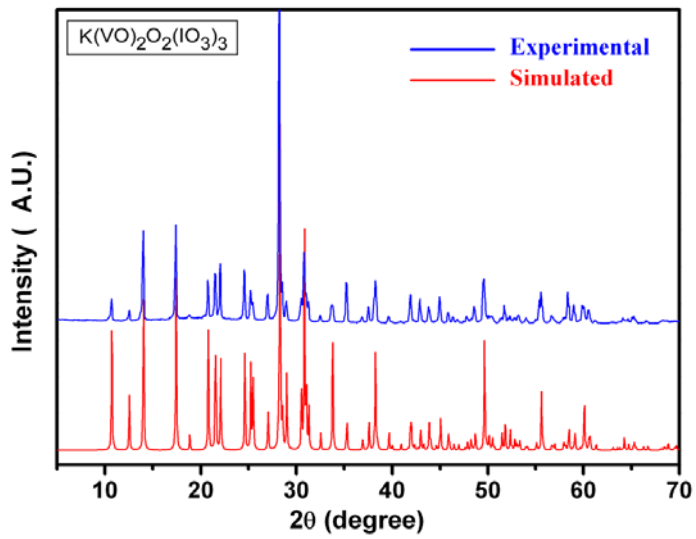
K(VO)2O2(IO3)3
Experimental
Simulated
Intensity (A.U.)
10
20
30
40
50
60
70
2θ (degree)

(d)

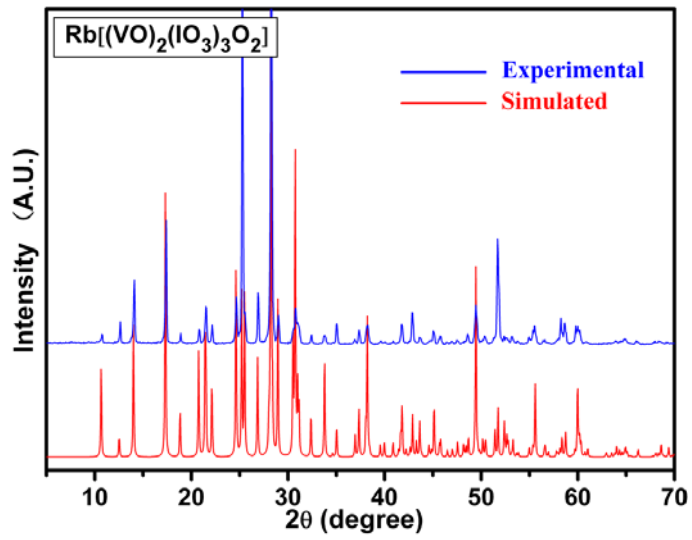
Rb[(VO)2(IO3)3O2]
Experimental
Simulated
Intensity (A.U.)
10
20
30
40
50
60
70
2θ (degree)

(e)

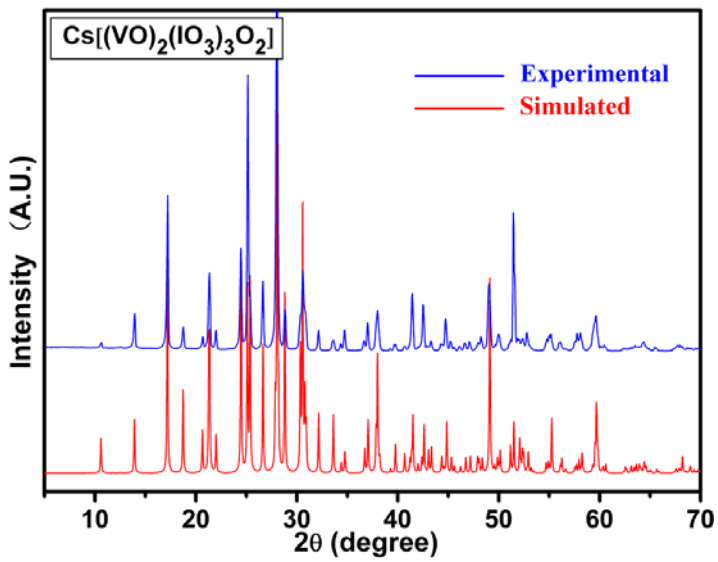
Cs[(VO)2(IO3)3O2]
Experimental
Simulated
Intensity (A.U.)
10
20
30
40
50
60
70
2θ (degree)

(f)

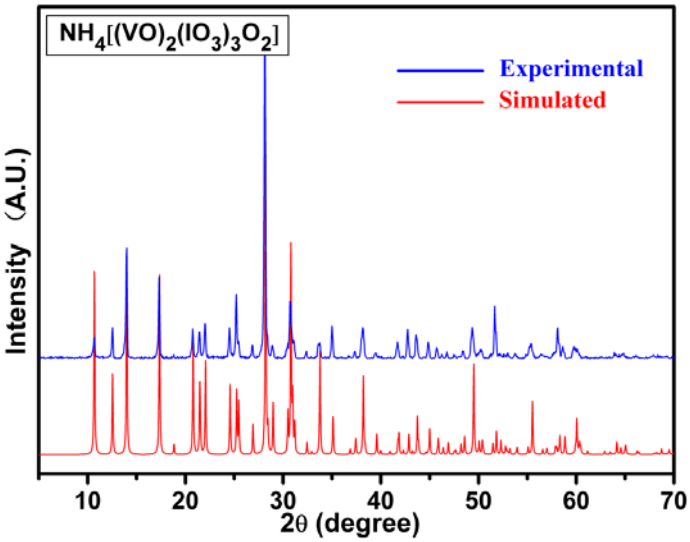

(g)

Figure S1. Experimental and simulated powder X-ray diffraction patterns for α-$KVO_2(IO_3)_2(H_2O)$, β-$KVO_2(IO_3)_2(H_2O)$, $K_4[(VO)(IO_3)_5]_2(HIO_3)(H_2O)_2{\cdot}H_2O$, $K(VO)_2O_2(IO_3)_3$, and $M[(VO)_2(IO_3)_3O_2]$ ($M = Rb^+$, Cs^+, NH_4^+).

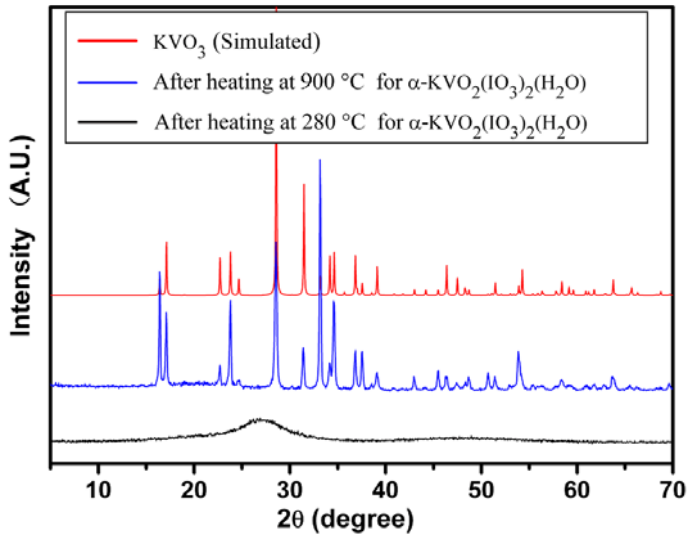
KVO3 (Simulated)
After heating at 900 °C for α-KVO2(IO3)2(H2O)
After heating at 280 °C for α-KVO2(IO3)2(H2O)
Intensity (A.U.)
10
20
30
40
50
60
70
2θ (degree)

(a)

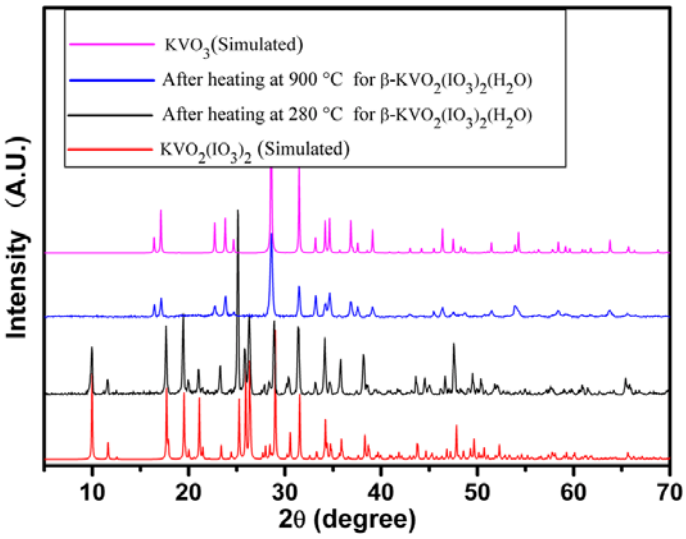
KVO3(Simulated)
After heating at 900 °C for β-KVO2(IO3)2(H2O)
After heating at 280 °C for β-KVO2(IO3)2(H2O)
KVO2(IO3)2 (Simulated)
Intensity (A.U.)
10
20
30
40
50
60
70
2θ (degree)

(b)

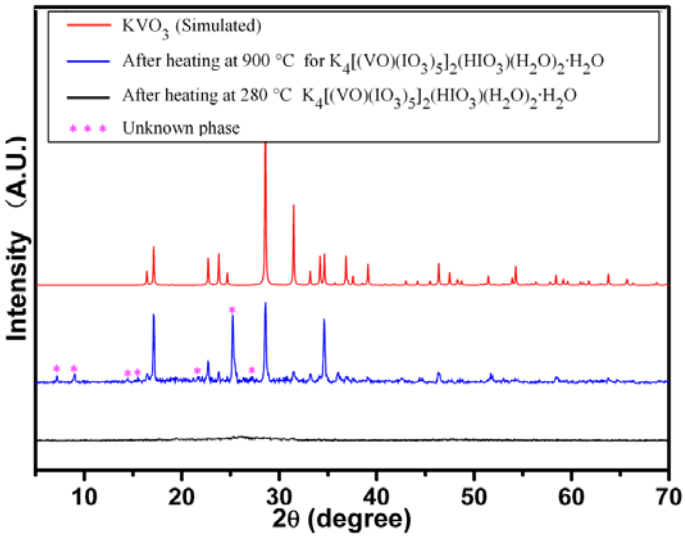
KVO3 (Simulated)
After heating at 900 °C for K4[(VO)(IO3)5]2(HIO3)(H2O)2·H2O
After heating at 280 °C K4[(VO)(IO3)5]2(HIO3)(H2O)2·H2O
Unknown phase
Intensity (A.U.)
10
20
30
40
50
60
70
2θ (degree)

(c)

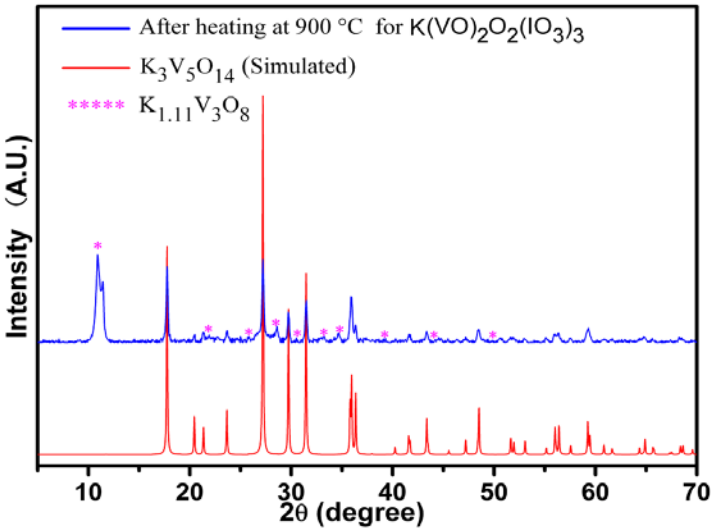

(d)

Figure S2. Powder X-ray diffraction patterns for the thermal decomposition residuals of α-$KVO_2(IO_3)_2(H_2O)$ (a), β-$KVO_2(IO_3)_2(H_2O)$ (b), $K_4[(VO)(IO_3)_5]_2(HIO_3)(H_2O)_2{\cdot}H_2O$ (c), and $K(VO)_2O_2(IO_3)_3$ (d).

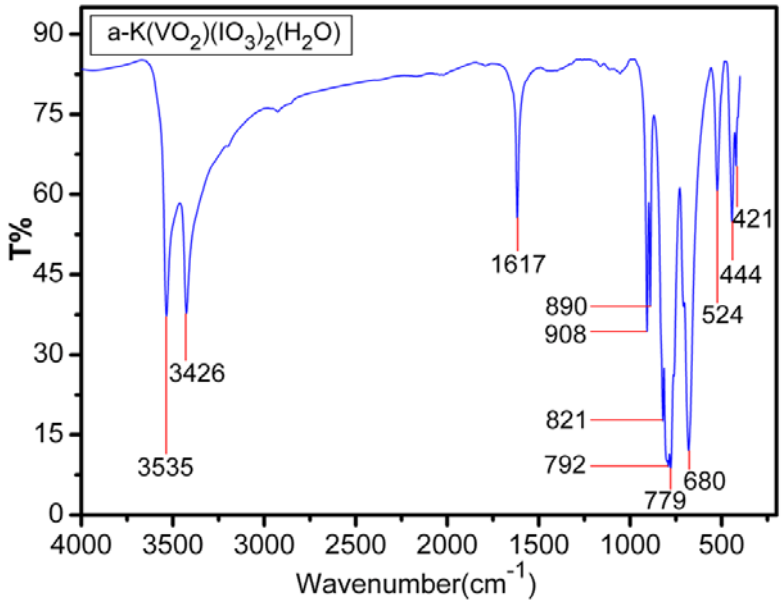
a-K(VO2)(IO3)2(H2O)
T%
Wavenumber(cm-1)
3535
3426
1617
890
908
821
792
779
680
524
444
421

(a)

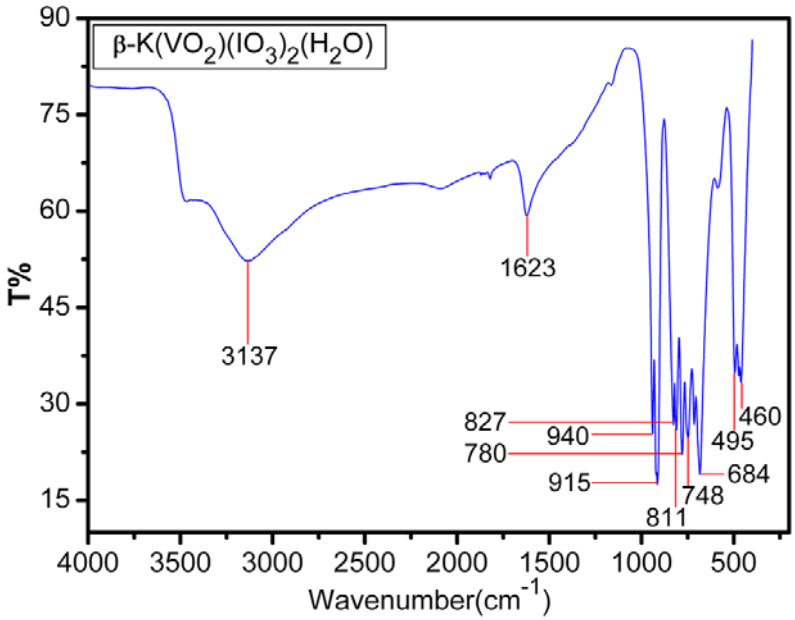
β-K(VO2)(IO3)2(H2O)
T%
Wavenumber(cm-1)
3137
1623
827
940
780
915
811
748
684
495
460

(b)

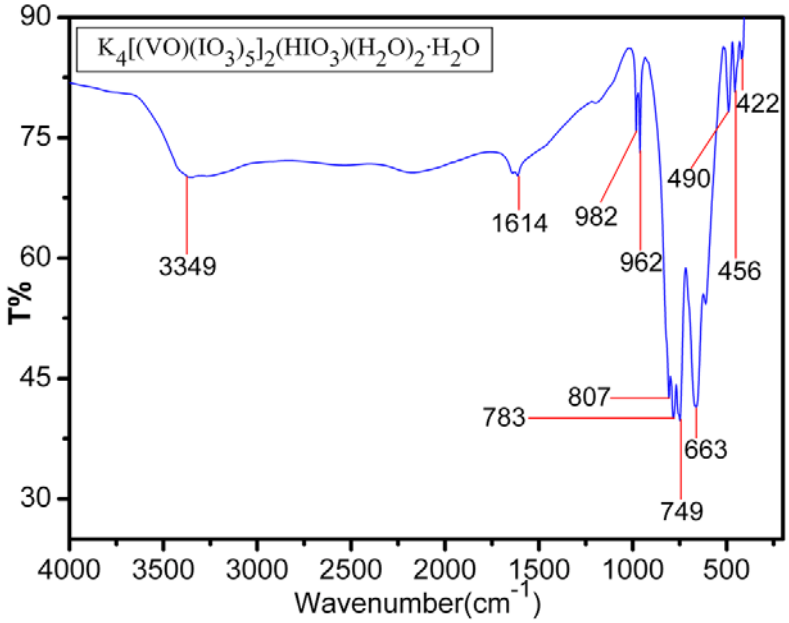

(c)

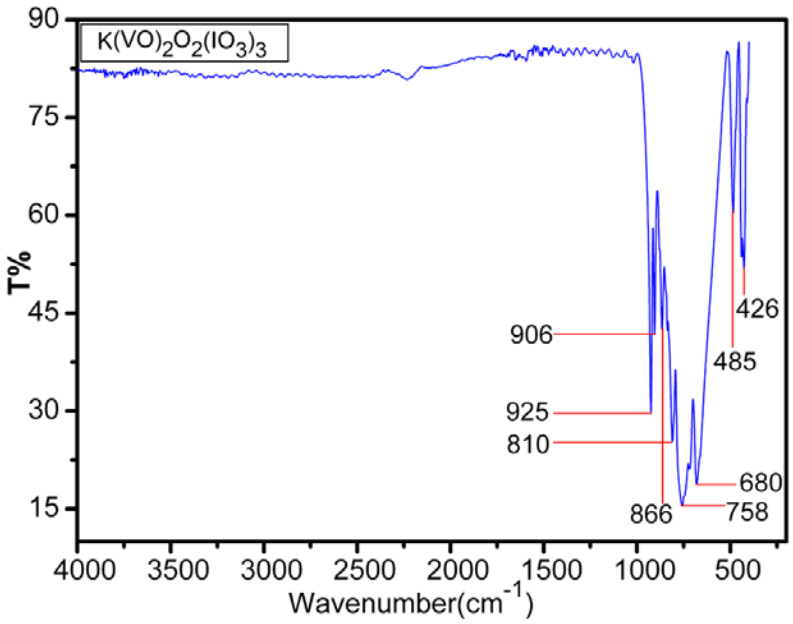

(d)

Figure S3. The infrared spectra of α-$KVO_2(IO_3)_2(H_2O)$ (a), β-$KVO_2(IO_3)_2(H_2O)$ (b), $K_4[(VO)(IO_3)_5]_2(HIO_3)(H_2O)_2{\cdot}H_2O$ (c), and $K(VO)_2O_2(IO_3)_3$ (d).

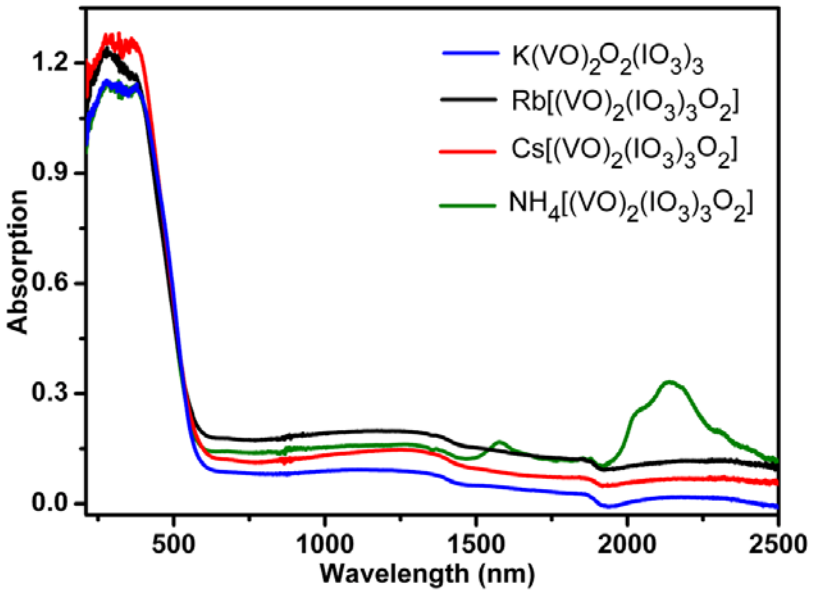

Figure S4. UV absorption spectra of $K(VO)_2O_2(IO_3)_3$ and $M[(VO)_2(IO_3)_3O_2]$ (M = Rb^+, Cs^+, NH_4^+).

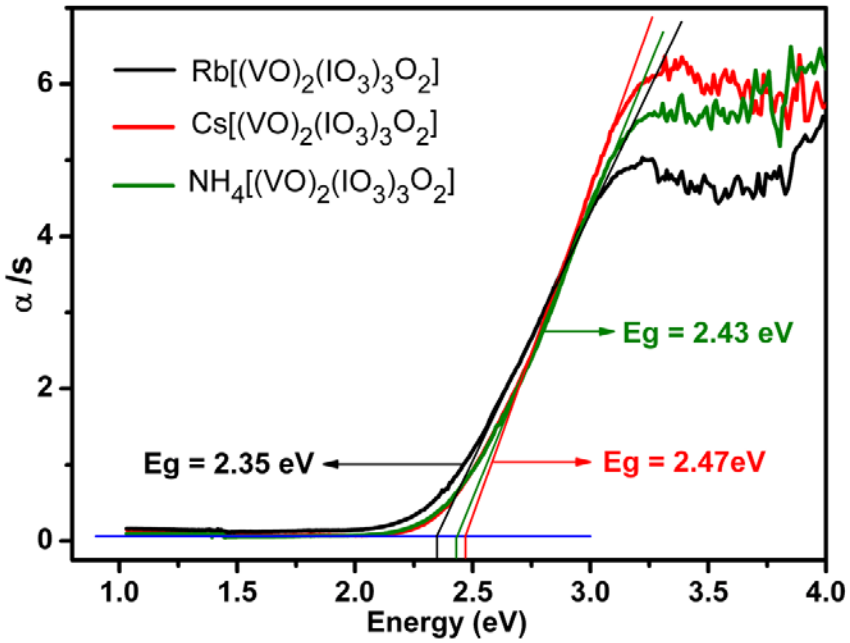

Figure S5. Optical diffuse reflectance spectra for $M[(VO)_2(IO_3)_3O_2]$ ($M = Rb^+$, Cs^+, NH_4^+).

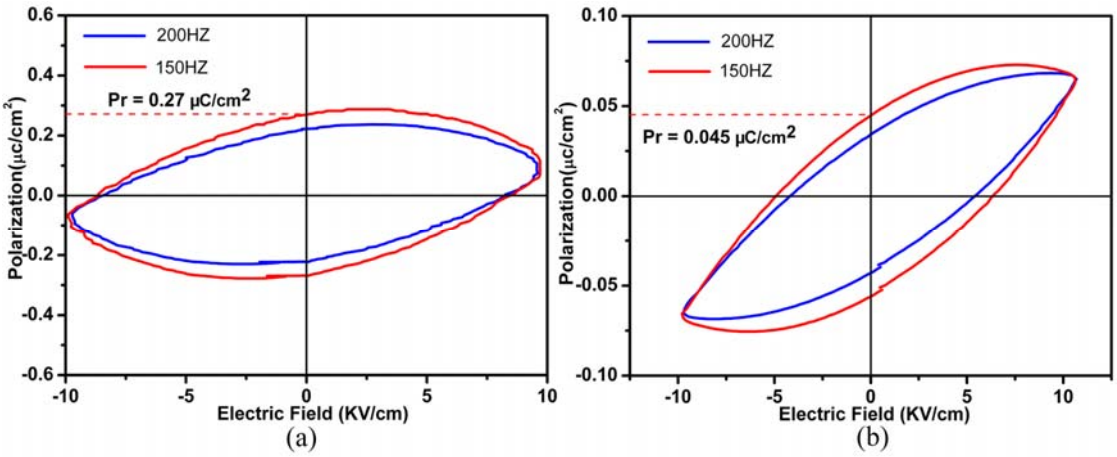

Figure S6. Polarization versus applied electric field for $K_4[(VO)(IO_3)_5]_2(HIO_3)(H_2O)_2{\cdot}H_2O$ (a) and $K(VO)_2O_2(IO_3)_3$ (b).

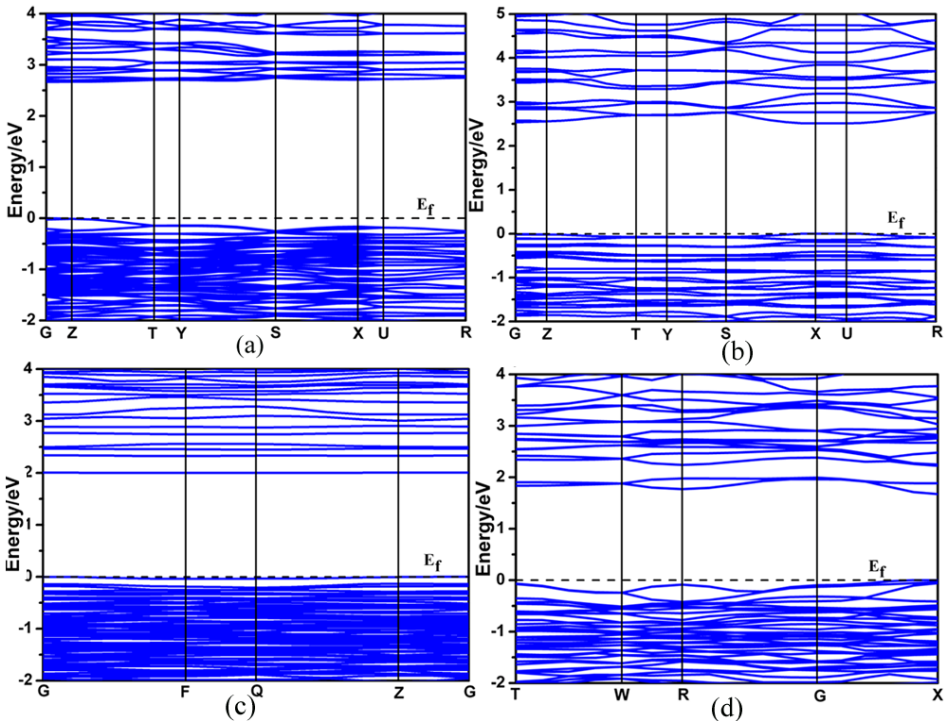

Figure S7. Calculated band structures of α-$KVO_2(IO_3)_2(H_2O)$ (a), β-$KVO_2(IO_3)_2(H_2O)$ (b), $K_4[(VO)(IO_3)_5]_2(HIO_3)(H_2O)_2{\cdot}H_2O$ (c), and $K(VO)_2O_2(IO_3)_3$ (d) (the Fermi level is set at 0 eV).

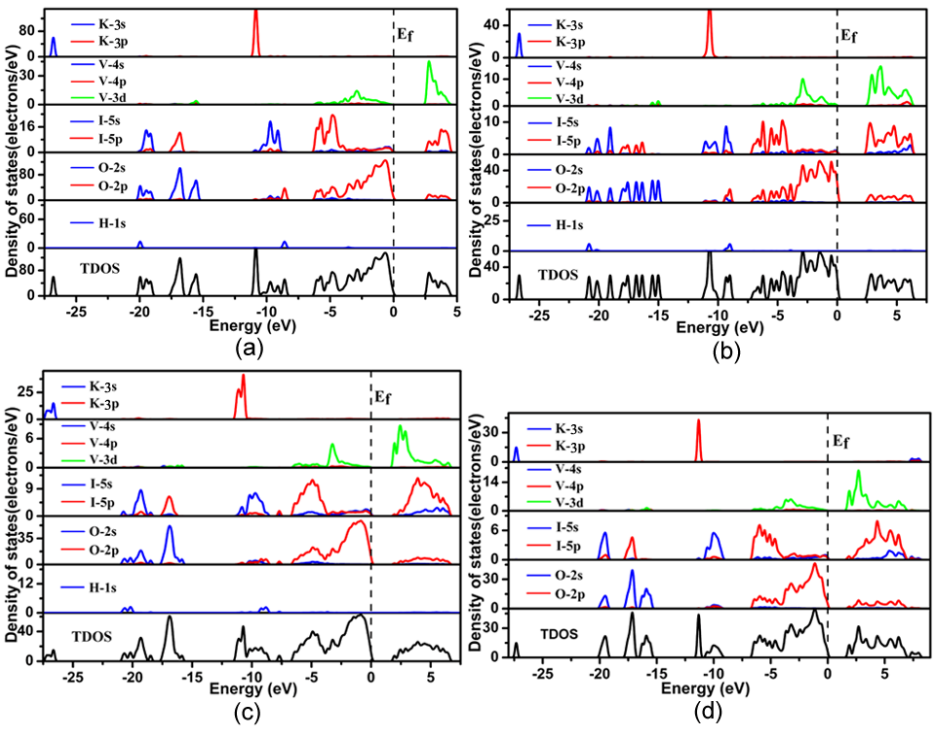

Figure S8. Electronic density of states of α-$KVO_2(IO_3)_2(H_2O)$ (a), β-$KVO_2(IO_3)_2(H_2O)$ (b), $K_4[(VO)(IO_3)_5]_2(HIO_3)(H_2O)_2{\cdot}H_2O$ (c), and $K(VO)_2O_2(IO_3)_3$ (d).

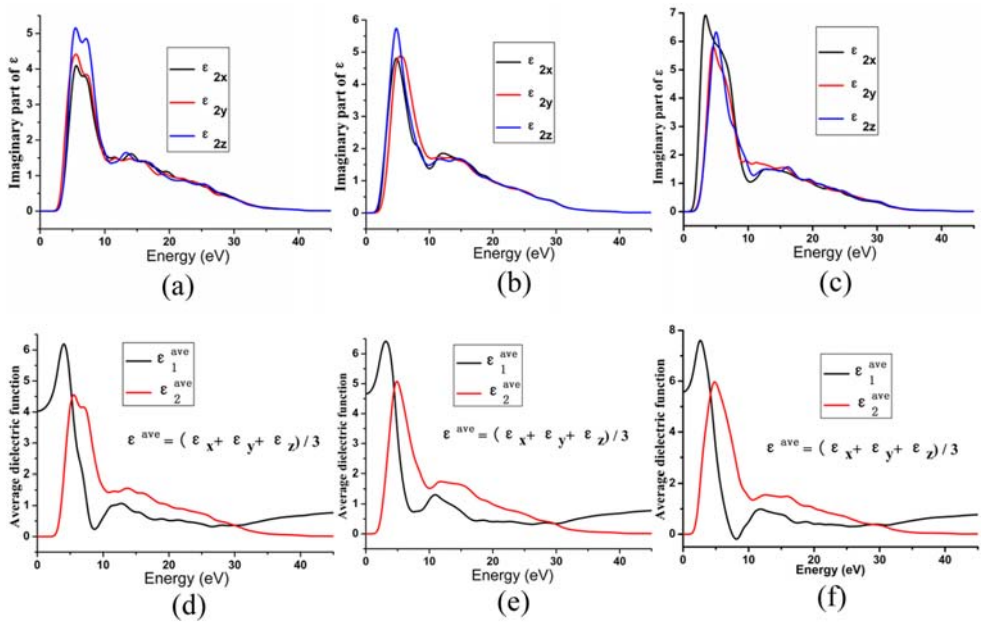

Figure S9. The imaginary part of the dielectric function polarized along three dielectric axes directions for β-$KVO_2(IO_3)_2(H_2O)$ (a), $K_4[(VO)(IO_3)_5]_2(HIO_3)(H_2O)_2{\cdot}H_2O$ (b), and $K(VO)_2O_2(IO_3)_3$ (c); and average imaginary part and real part of the dielectric function over three dielectric axes directions β-$KVO_2(IO_3)_2(H_2O)$ (d), $K_4[(VO)(IO_3)_5]_2(HIO_3)(H_2O)_2{\cdot}H_2O$ (e), and $K(VO)_2O_2(IO_3)_3$ (f).

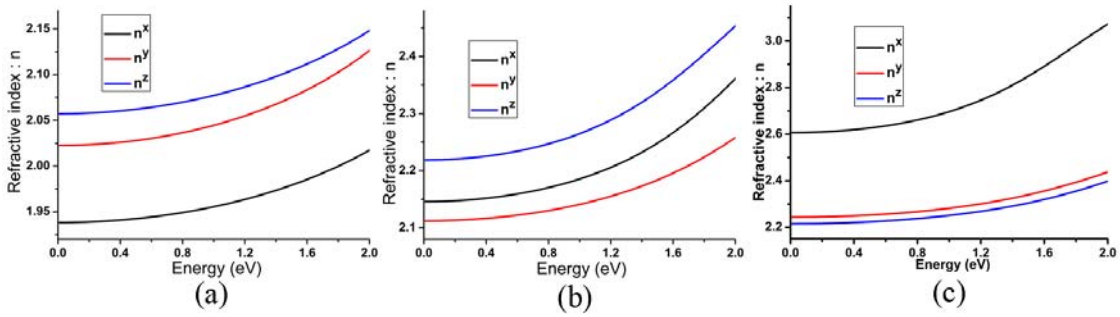

Figure S10. Calculated linear refractive indices for β-$KVO_2(IO_3)_2(H_2O)$ (a), $K_4[(VO)(IO_3)_5]_2(HIO_3)(H_2O)_2{\cdot}H_2O$ (b), and $K(VO)_2O_2(IO_3)_3$ (c).

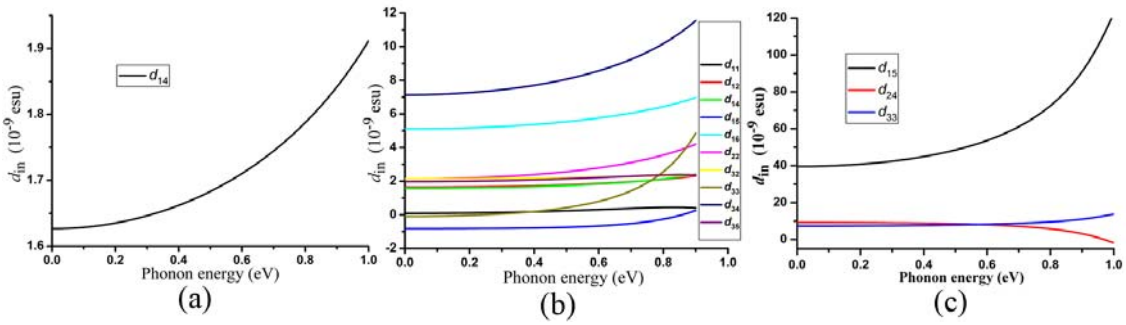

Figure S11. Calculated frequency-dependent second harmonic generation coefficients for β-$KVO_2(IO_3)_2(H_2O)$ (a), $K_4[(VO)(IO_3)_5]_2(HIO_3)(H_2O)_2{\cdot}H_2O$ (b), and $K(VO)_2O_2(IO_3)_3$ (c).

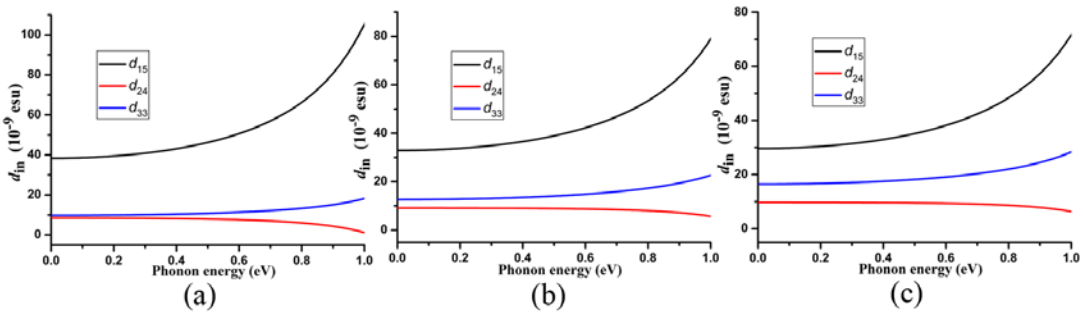

Figure S12. Calculated frequency-dependent second harmonic generation coefficients for $Rb[(VO)_2(IO_3)_3O_2]$ (a), $Cs[(VO)_2(IO_3)_3O_2]$ (b), and $NH_4[(VO)_2(IO_3)_3O_2]$ (c).